Chapter 5

IRS-Assisted Downlink NOMA System

In this Chapter, BER performance of an IRS-assisted downlink NOMA system is analyzed by considering SIC errors. The IRS-assisted NOMA system is assumed to experience independent and nonidentically distributed (i.n.i.d.) Rician fading channels. Closed-form BER expressions for each user in the IRS-assisted NOMA system are derived.

5.1 Introduction

The ever-evolving landscape of wireless communication has given rise to IRS, a cost-effective solution revolutionizing service quality [15, 84]. These remarkable surfaces employ cutting-edge beamforming techniques to deftly redirect incoming signals, unleashing a powerful combination of extended coverage and heightened energy efficiency across wireless networks. In parallel, NOMA has emerged as a formidable

contender, empowering multiple users to seamlessly share resources through signal superposition, elevating spectral efficiency to new heights [110]. It is in the seamless fusion of IRS and NOMA that we find the potential to unlock untapped realms of energy and spectral efficiencies, defining the future of modern wireless networks.

The performance analysis of wireless communication systems incorporating NOMA or/and IRS has been done in [5, 20, 21, 29, 37–44]. The BER performance of NOMA has been studied assuming imperfect SIC in [18, 37]. Additionally, a simplified design of IRS-assisted NOMA (INOMA) has been proposed and analyzed in [5, 45]. The power-efficient aspects of INOMA have been explored in [21, 38], where joint optimization of beamforming vectors and IRS phase shift matrices aims to enhance the sum-rate performance. The OP analysis of INOMA under perfect and imperfect SIC is studied in [39]. Furthermore, the OP analysis of IRS-assisted uplink NOMA under Nakagami-m fading, utilizing moments matching, has been investigated in [40]. The OP analysis for multi-antenna IRS-assisted NOMA, considering both discrete and continuous phases, has derived in [41]. Additionally, a near-optimal solution is obtained using semi-definite relaxation for maximization of sum-rate for all users while adhering to constraints on individual power [42]. Another study [44] presents the BER performance of INOMA for various modulation schemes, including BPSK and quadrature phase shift keying (QPSK), across different fading channels using only Monte Carlo simulations.

Contributions: The BER performance of the IRS-assisted downlink NOMA system (INOMA), considering Rician fading channels and the presence of SIC errors, has not been explored. The analysis of the INOMA system is both significant and intriguing, as it improves both the energy and spectral efficiencies of wireless networks. In this chapter, we have derived the BER expressions of IRS-aided downlink

power domain NOMA over independent and non-identically distributed (i.n.i.d.) Rician fading channels consider both near and far users. Specifically, we have adopted a modulation pair: QPSK for the near user and BPSK for the far user. The derived theoretical BER expressions have been validated through Monte Carlo simulations. Moreover, we have investigated the impact of various factors, such as the number of IRS elements, the location of the IRS panel, the Rician factor, and power coefficient variation, on the BER performance of the proposed downlink INOMA system.

The rest of the chapter is structured as follows. Section 5.2 presents the system and channel models. The BER expressions are derived in Section 5.3. The simulation and numerical results are discussed in Section 5.4. Finally, Section 5.5 summarizes the chapter.

5.2 System and Channel Models

The system configuration shown in Figure 5.1 depicts a two-user-based INOMA system, in which direct links between the BS and the users are blocked, and each user is assisted by a separate IRS panel. Both IRS panels are positioned in the LoS of the BS and the respective users. The IRS-1 consists of N_{n} reflecting elements allocated to the near user, while the IRS-2 has N_{f} reflecting elements assigned to the far user. Each IRS panel redirects the received signal towards its corresponding user, as illustrated in Figure 5.1. Further, it is assumed that perfect CSI is available at the IRS panels. The received signal r_{u} at the user $\mathrm{u} \in \{\mathrm{n}, \mathrm{f}\}$ can be mathematically expressed as follows:

$$r_{\mathrm{u}} = \sqrt{P_{\mathrm{t}}} \left(\mathbf{g}_{\mathrm{u}}^{T} \mathbf{\Theta}_{\mathrm{u}} \mathbf{h}_{\mathrm{r}} \right) S_{\mathrm{sc}} + n_{\mathrm{u}}, \qquad \mathrm{u} \in \{\mathrm{n}, \mathrm{f}\} \tag{5.1}$$

where r_{n} and r_{f} denote the received signal at the near and far user, respectively. P_{t} is the total transmit power of superposition coded message signal S_{sc} at the BS. $\mathbf{h}_{\mathrm{u}} = [h_{u1}, h_{u2}, \ldots h_{uN_u}]$ and $\mathbf{g}_{\mathrm{u}} = [g_{u1}, g_{u2}, \ldots g_{uN_u}]$ are the vectors of channel coefficients between the BS to IRS, and IRS to the user $\mathrm{u} \in \{\mathrm{n}, \mathrm{f}\}$, respectively. $\mathbf{\Theta}_{\mathrm{u}} = \mathrm{diag}\{[e^{j\theta_{u1}}, e^{j\theta_{u2}}, ..., e^{j\theta_{uN_u}}]\}$ is a diagonal matrix that contains the phase shifts

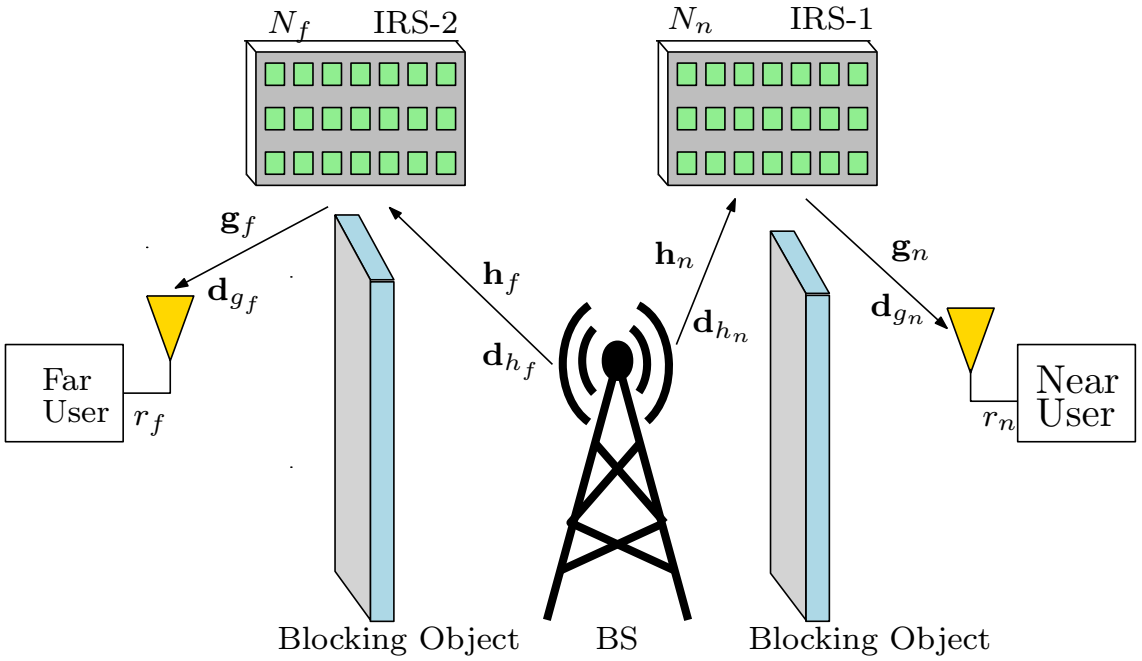

FIGURE 5.1: Two users IRS-assisted downlink power domain NOMA communication system.

applied by the reflecting surfaces of the IRS panel. It is assumed that the reflection coefficient is unity and $\theta_{uN_u} \in [0, 2\pi)$ for $\mathrm{u} \in \{\mathrm{n}, \mathrm{f}\}$. The term n_{u} denotes the AWGN with zero mean and variance N_0 at the user u. The superposition-coded message signal S_{sc} at the BS is represented as

$$S_{\mathrm{sc}} = \sqrt{\epsilon_{\mathrm{n}}}\, s_{\mathrm{n}} + \sqrt{\epsilon_{\mathrm{f}}}\, s_{\mathrm{f}}, \tag{5.2}$$

where ϵ_{n} and ϵ_{f} represent the symbol energies of the near user n and far user f, respectively. Specifically, these can be represented as $\epsilon_{\mathrm{n}} = \alpha P_t$ and $\epsilon_{\mathrm{f}} = (1-\alpha)P_t$. s_{n} and s_{f} are the modulated symbols for near user and far user, respectively.

The placement of the IRS panels is such that they are positioned in the LoS of both the users and the BS. The h_{ui} ($(1 \leq i \leq N_u$ and $\mathrm{u} \in \{\mathrm{n}, \mathrm{f}\}$) denote the channel between the BS and the IRS panel corresponding to user u. Thus, h_{ui} is modeled as a Rician distribution with non-identical Rician parameters K_{h_u}. The distance between the BS and the IRS panel corresponding to user u is denoted by d_{h_u}, and the path loss exponent is denoted by α_{h_u}.

Similarly, the channel coefficients between the IRS panel and user u are represented by g_{ui} ($(1 \leq i \leq N_\mathrm{m}$ u $\in \{\mathrm{n}, \mathrm{f}\}$). The g_{ui} channel is also modeled as a Rician distribution with non-identical Rician parameter denoted by K_{g_u}. The distance between the IRS panel and the user u is denoted by d_{g_u} , and the path loss exponent is denoted by α_{g_u}.

The PDF of RV $|v| \in \{|h_{ui}|, |g_{ui}|\}$ is modeled by a Rician distribution with the Rician parameter $K_v \in \{K_{h_\mathrm{u}}, K_{g_\mathrm{u}}\}$. The PDF of $|v|$ is given as

$$f_{|v|}(v) = \frac{2(1+K_v)v}{\exp\left(K_v\right)\Omega_v} \exp\left(-\frac{(1+K_v)v^2}{\Omega_v}\right) \times I_0\left(2v\sqrt{\frac{K_v(1+K_v)}{\Omega_v}}\right), \qquad v \geq 0 \tag{5.3}$$

where $\Omega_v = d_v^{-\alpha_v} \in \{d_{h_u}^{-\alpha_{h_u}}, d_{\mathrm{g}_u}^{-\alpha_{\mathrm{g}_u}}\}$. Now, we assume that $z_\mathrm{u} = \sum_{i=1}^{N_\mathrm{u}} |h_{ui}|\,|g_{ui}|$ is the end-to-end channel gain of the user u (where $\mathrm{u} \in \{\mathrm{n}, \mathrm{f}\}$) from the BS via the IRS panel. Furthermore, we assume that the channel gains between the BS and the individual users satisfy the condition $\mathbb{E}\{|z_\mathrm{n}|^2\} \geq \mathbb{E}\{|z_\mathrm{f}|^2\}$, where $\mathbf{E}\{\cdot\}$ denotes statistical averaging.

For analytical analysis, the instantaneous SNR of user u is given by $\gamma_\mathrm{u}{=}|z_\mathrm{u}|^2 \left(\frac{\epsilon_\mathrm{u}}{N_0}\right)$, where ϵ_u is the average energy of constellation point s_u. Since $|h_{ui}|$ and $|g_{ui}|$ are independent Rician distributed RVs and the number of reflecting elements N_u is

sufficiently large ($N_{\mathrm{u}} >> 1$), we can apply the central limit theorem. As a result, the RV $z_{\mathrm{u}} = \sum_{i=1}^{N_{\mathrm{u}}} z_{ui} = \sum_{i=1}^{N_{\mathrm{u}}} |h_{ui}|\,|g_{ui}|$ can be modeled as a normally distributed RV with the following mean μ_{u} and variance σ_{u}^2 [35]:

$$\mu_{\mathrm{u}} = \frac{N_{\mathrm{u}}\,\pi\,L_{0.5}\left(-K_{h_{\mathrm{u}}}\right)L_{0.5}\left(-K_{g_{\mathrm{u}}}\right)}{4\sqrt{d_{h_{\mathrm{u}}}^{\alpha_{h_{\mathrm{u}}}}\,d_{g_{\mathrm{u}}}^{\alpha_{g_{\mathrm{u}}}}\left(K_{h_{\mathrm{u}}}+1\right)\left(K_{g_{\mathrm{u}}}+1\right)}}, \tag{5.4}$$

$$\sigma_{\mathrm{u}}^2 = \frac{N_{\mathrm{u}}}{d_{h_{\mathrm{u}}}^{\alpha_{h_{\mathrm{u}}}}\,d_{g_{\mathrm{u}}}^{\alpha_{g_{\mathrm{u}}}}}\left[1 - \frac{\pi^2\,L_{0.5}^2\left(-K_{h_{\mathrm{u}}}\right)L_{0.5}^2\left(-K_{g_{\mathrm{u}}}\right)}{16\left(K_{h_{\mathrm{u}}}+1\right)\left(K_{g_{\mathrm{u}}}+1\right)}\right], \tag{5.5}$$

where the Laguerre polynomial of degree j is represented by $L_j(\cdot)$. Therefore, the RV γ_{u} follows a non-central chi-square distribution with one degree of freedom, and its MGF is given by [29, 35] Hence, the RV γ_{u} is a non-central chi-square RV with one degree of freedom and has the following MGF [29, 35]

$$M_{\gamma_u}(s) \approx \left(\frac{\Delta_{u1}}{\Delta_{u1} - s\epsilon_u\gamma_0}\right)^{0.5} \exp\left(-\frac{s\epsilon_u\gamma_0\Delta_{u2}}{\Delta_{u1} - s\epsilon_u\gamma_0}\right), \tag{5.6}$$

where s denotes the Laplace variable, $\gamma_0 = \frac{1}{N_0}$, $\Delta_{u1} = \frac{1}{\sigma_{\mathrm{u}}^2}$ and $\Delta_{u2} = \frac{\mu_{\mathrm{u}}^2}{2\sigma_{\mathrm{u}}^2}$.

5.3 BER Analysis of Downlink NOMA

The BER $P_{\mathrm{u}}(e)$ of user $\mathrm{u} \in \{\mathrm{n}, \mathrm{f}\}$ for the considered downlink INOMA can be obtained by averaging the conditional BER over the PDF $f_{\gamma_{\mathrm{u}}}(\cdot)$ of the instantaneous SNR γ_{u} of user u [37], i.e.,

$$P_{\mathrm{u}}(e) = \mathbb{E}\left[P(e|\gamma_{\mathrm{u}})\right], \tag{5.7}$$

where $P(e|\gamma_{\mathrm{u}})$ represents the conditional BER of a digital modulation scheme for the user $\mathrm{u} \in \{\mathrm{n}, \mathrm{f}\}$. Note that we have considered the QPSK modulation scheme for near user n and the BPSK modulation scheme for the far user f in the INOMA.

5.3.1 Accurate BER Expression for $N_{\mathrm{u}} >> 1$

5.3.1.1 BER Expression for Far User f

For the far user, utilizing the expression from [37, (7)], the conditional BER can be represented as

$$P(e|\gamma_{\mathrm{f}}) = \frac{1}{2}Q\left(\sqrt{\gamma_{\mathrm{f}}^{(1)}}\right) + \frac{1}{2}Q\left(\sqrt{\gamma_{\mathrm{f}}^{(2)}}\right), \tag{5.8}$$

where $\gamma_{\mathrm{f}}^{(1)} = \frac{\left(\sqrt{2\epsilon_{\mathrm{f}}}+\sqrt{\epsilon_{\mathrm{n}}}\right)^2}{N_0}|z_{\mathrm{f}}|^2$, and $\gamma_{\mathrm{f}}^{(2)} = \frac{\left(\sqrt{2\epsilon_{\mathrm{f}}}-\sqrt{\epsilon_{\mathrm{n}}}\right)^2}{N_0}|z_{\mathrm{f}}|^2$. Substituting (5.8) into (5.7) and using alternate Q-function $\left(Q(t) = \frac{1}{\pi}\int_0^{\pi/2}\exp\left(\frac{-t^2}{2\sin^2\varphi}\right)d\varphi\right)$, the BER expression of the far user f is given by

$$P_{\mathrm{f}}(e) = \frac{1}{2}\mathcal{I}_{\mathrm{f}}^{(1)}\left(\frac{\pi}{2}\right) + \frac{1}{2}\mathcal{I}_{\mathrm{f}}^{(2)}\left(\frac{\pi}{2}\right), \tag{5.9}$$

where the $\mathcal{I}_{\mathrm{f}}^{(j)}(\frac{\pi}{2})$ can be expressed as

$$\begin{aligned}
\mathcal{I}_{\mathrm{f}}^{(j)}\left(\frac{\pi}{2}\right) &= \mathbf{E}\left[Q\left(\sqrt{\gamma_{\mathrm{f}}^{(j)}}\right)\right], \qquad j = 1, 2. \\
&= \int_0^{\infty} Q\left(\sqrt{\gamma_{\mathrm{f}}^{(j)}}\right) f_{\gamma_{\mathrm{f}}^{(j)}}\left(\gamma_{\mathrm{f}}^{(j)}\right) d\gamma_{\mathrm{f}}^{(j)} \\
&= \frac{1}{\pi}\int_0^{\frac{\pi}{2}}\int_0^{\infty} \exp\left(\frac{-\gamma_{\mathrm{f}}^{(j)}}{2\sin^2\varphi}\right) f_{\gamma_{\mathrm{f}}^{(j)}}\left(\gamma_{\mathrm{f}}^{(j)}\right) d\gamma_{\mathrm{f}}^{(j)}\, d\varphi \\
&= \frac{1}{\pi}\int_0^{\frac{\pi}{2}} \mathcal{M}_{\gamma_{\mathrm{f}}^{(j)}}\left(\frac{1}{2\sin^2\varphi}\right) d\varphi,
\end{aligned} \tag{5.10}$$

where the MGF expression $M_{\gamma_{\mathrm{f}}^{(j)}}(s)$ of far user having SNR $\gamma_{\mathrm{f}}^{(j)}$ is given with the aid of (5.6). To achieve a closed-form solution for the BER expression $P_{\mathrm{f}}(e)$, it is necessary to obtain a solution for the integral $\mathcal{I}_{\mathrm{f}}^{(j)}\left(\frac{\pi}{2}\right)$, as provided in the Appendix C.

5.3.1.2 BER Expression for Near User n

For the near user, the conditional BER expression taking SIC errors into account can be written as [37, (23)]

$$P_{\mathrm{n}}(e|\gamma_{\mathrm{n}}) = Q\left(\sqrt{\gamma_{\mathrm{n}}^{(1)}}\right) + \frac{1}{4}\left[-Q\left(\sqrt{\gamma_{\mathrm{n}}^{(2)}}\right) + Q\left(\sqrt{\gamma_{\mathrm{n}}^{(3)}}\right) + Q\left(\sqrt{\gamma_{\mathrm{n}}^{(4)}}\right) - Q\left(\sqrt{\gamma_{\mathrm{n}}^{(5)}}\right)\right], \tag{5.11}$$

where $\gamma_{\mathrm{n}}^{(1)} = \frac{\epsilon_{\mathrm{n}}}{N_0}|z_{\mathrm{n}}|^2$, $\gamma_1^{(2)} = \frac{\left(\sqrt{2\epsilon_{\mathrm{f}}}+\sqrt{\epsilon_{\mathrm{n}}}\right)^2}{N_0}|z_{\mathrm{n}}|^2$, $\gamma_{\mathrm{n}}^{(3)} = \frac{\left(\sqrt{2\epsilon_{\mathrm{f}}}-\sqrt{\epsilon_{\mathrm{n}}}\right)^2}{N_0}|z_{\mathrm{n}}|^2$, $\gamma_{\mathrm{n}}^{(4)} = \frac{\left(2\sqrt{2\epsilon_{\mathrm{f}}}+\sqrt{\epsilon_{\mathrm{n}}}\right)^2}{N_0}|z_{\mathrm{n}}|^2$, and $\gamma_{\mathrm{n}}^{(5)} = \frac{\left(2\sqrt{2\epsilon_{\mathrm{n}}}-\sqrt{\epsilon_{\mathrm{f}}}\right)^2}{N_0}|z_{\mathrm{n}}|^2$. Substituting (5.11) into (5.7) and using the alternate expression of the Q-function, the BER expression of the near user is given by

$$P_{\mathrm{n}}(e) = \mathcal{I}_{\mathrm{n}}^{(1)}\left(\frac{\pi}{2}\right) + \frac{1}{4}\left[-\mathcal{I}_{\mathrm{n}}^{(2)}\left(\frac{\pi}{2}\right) + \mathcal{I}_{\mathrm{n}}^{(3)}\left(\frac{\pi}{2}\right) + \mathcal{I}_{\mathrm{n}}^{(4)}\left(\frac{\pi}{2}\right) - \mathcal{I}_{\mathrm{n}}^{(5)}\left(\frac{\pi}{2}\right)\right], \tag{5.12}$$

where $\mathcal{I}_{\mathrm{n}}^{(j)}\left(\frac{\pi}{2}\right)$ is defined as similar to $\mathcal{I}_{\mathrm{n}}^{(j)}\left(\frac{\pi}{2}\right)$, i.e.,

$$\begin{aligned}\mathcal{I}_{\mathrm{n}}^{(j)}\left(\frac{\pi}{2}\right) &= \mathbf{E}\left[Q\left(\sqrt{\gamma_{\mathrm{n}}^{(j)}}\right)\right], \qquad j = 1,2,3,4,5 \\ &= \frac{1}{\pi}\int_0^{\frac{\pi}{2}} M_{\gamma_{\mathrm{n}}^{(j)}}\Big(\frac{1}{2\sin^2\varphi}\Big)d\varphi,\end{aligned} \tag{5.13}$$

where the MGF expression $M_{\gamma_{\mathrm{n}}^{(j)}}(s)$ of near user n having SNR $\gamma_{\mathrm{n}}^{(j)}$ is given by using (5.6). Note that a solution of the integral $\mathcal{I}_{\mathrm{n}}^{(j)}\left(\frac{\pi}{2}\right)$ is provided in Appendix C.

5.3.2 Asymptotic BER Expressions

In this section, asymptotic BER is derived by considering $\gamma_{\mathrm{u}} \to \infty$. First, we will derive Asymptotic MGF.

5.3.2.1 Asymptotic MGF for γ_{u}

When the arguments of the Bessel function are small, the relation $I_0(z) \approx 1$ holds [75, (9.6.7)]. Utilizing this relation in (5.3), and performing some algebraic simplifications, the asymptotic PDF expression of $v \in |h_{ui}|, |g_{ui}|$ can be expressed as

$$f_{|v|}^{\infty}(v) \approx \mathcal{A}_v \, v \, \exp\left(-\mathcal{B}_v v^2\right), \quad v \geq 0 \tag{5.14}$$

where $\mathcal{A}_v = \frac{2(1+K_v)}{\exp(K_v)\Omega_v}$ and $\mathcal{B}_v = \frac{(1+K_v)}{\Omega_v}$. Now, using [79, (2.3.16.1)], the asymptotic PDF expression of $z_{ui} = |h_{ui}|\,|g_{ui}|$ can be obtain

$$\begin{aligned} f_{z_{ui}}^{\infty}(z) &= \int_0^{\infty} \frac{1}{h} f_{|h_{ui}|}(h)\, f_{|g_{ui}|}\left(\frac{z}{h}\right) dh \\ &= \mathcal{A}_{h_{ui}} \mathcal{A}_{g_{ui}}\, z\, K_0\left(2z\sqrt{\mathcal{B}_{h_{ui}}\mathcal{B}_{g_{ui}}}\right) \quad z \geq 0 \end{aligned} \tag{5.15}$$

Once more, for a small argument of the modified second kind Bessel function $K_0(\cdot)$, we can approximate the asymptotic PDF expression of z_{ui} in (5.15) as [1]

$$f_{z_{ui}}^{\infty}(z) \approx \Delta\, \mathcal{A}_{h_{ui}} \mathcal{A}_{g_{ui}} z \quad z \geq 0 \tag{5.16}$$

[1] Please take note that we have excluded the $-\ln z$ term in the approximation.

where $\Delta = -\lim_{\Omega_h \Omega_g \to \infty} \ln\left(\mathcal{B}_{h_{ui}} \mathcal{B}_{g_{ui}}\right)$ and $\ln(\cdot)$ denotes the natural logarithm. Therefore, the asymptotic MGF of z_{ui} can be given by

$$\mathcal{M}_{z_{ui}}^{\infty}(s) = \mathcal{L}\left\{f_{z_{ui}}^{\infty}(z)\right\} \approx \Delta\, \mathcal{A}_{h_{ui}} \mathcal{A}_{g_{ui}}\; s^{-2}. \tag{5.17}$$

Since W_is are independent random variables, the asymptotic MGF of z_{u} can be written as

$$\mathcal{M}_{z_{\mathrm{u}}}^{\infty}(s) = \prod_{i=1}^{N-u} \mathcal{M}_{z_{ui}}^{\infty}(s) \approx \left(\prod_{i=1}^{N_{\mathrm{n}}} \Delta\, \mathcal{A}_{h_{ui}} \mathcal{A}_{g_{ui}}\right) s^{-2N_{\mathrm{u}}}. \tag{5.18}$$

By performing the inverse Laplace transform of (5.18), one can derive the asymptotic PDF expression of z_{u} as

$$f_{z_{\mathrm{u}}}^{\infty}(z) = \mathcal{L}^{-1}\left\{\mathcal{M}_{z_{\mathrm{u}}}^{\infty}(s)\right\} \approx \left(\prod_{i=1}^{N_{\mathrm{u}}} \Delta\, \mathcal{A}_{h_{ui}} \mathcal{A}_{g_{ui}}\right) \frac{z^{2N_{\mathrm{u}}-1}}{\Gamma(2N_{\mathrm{u}})}, \qquad z \geq 0 \tag{5.19}$$

Applying the transformation of random variables, the asymptotic PDF expression of γ_{u} can be expressed as

$$f_{\gamma_{\mathrm{u}}}^{\infty}(\gamma) \approx \left(\prod_{i=1}^{N_{\mathrm{u}}} \Delta\, \mathcal{A}_{h_{ui}} \mathcal{A}_{g_{ui}}\right) \frac{\gamma^{N_{\mathrm{u}}-1}}{2\Gamma(2N_{\mathrm{u}})\bar{\gamma}^{N_{\mathrm{u}}}}, \quad \gamma \geq 0 \tag{5.20}$$

where $\bar{\gamma} = \epsilon_{\mathrm{u}}/N_0$. By taking the Laplace transform of (5.20), we can derive the asymptotic MGF expression of γ as

$$\mathcal{M}_{\gamma_{\mathrm{u}}}^{\infty}(s) = \mathcal{L}\left\{f_{\gamma_{\mathrm{u}}}^{\infty}(\gamma)\right\} = \left(\prod_{i=1}^{N_{\mathrm{u}}} \Delta\, \mathcal{A}_{h_{ui}} \mathcal{A}_{g_{ui}}\right) \frac{\Gamma(N_{\mathrm{u}})}{2\Gamma(2N_{\mathrm{u}})\left(s\bar{\gamma}\right)^{N_{\mathrm{u}}}} \tag{5.21}$$

5.3.2.2 Asymptotic BER Expression for Far User f

For the far user f, the asymptotic BER expression can be given by

$$P_{\mathrm{f},\infty}(e) = \frac{1}{2}\mathcal{I}^{(1)}_{\mathrm{f},\infty}\left(\frac{\pi}{2}\right) + \frac{1}{2}\mathcal{I}^{(2)}_{\mathrm{f},\infty}\left(\frac{\pi}{2}\right), \tag{5.22}$$

where the $\mathcal{I}^{(j)}_{\mathrm{f},\infty}(\frac{\pi}{2})$ can be expressed as

$$\mathcal{I}^{(j)}_{\mathrm{f},\infty}\left(\frac{\pi}{2}\right) = \frac{1}{\pi}\int_0^{\frac{\pi}{2}} \mathcal{M}^{\infty}_{\gamma^{(j)}_{\mathrm{f}}}\Big(\frac{1}{2\sin^2\varphi}\Big)d\varphi, \tag{5.23}$$

where the asymptotic MGF expression $M^{\infty}_{\gamma^{(j)}_{\mathrm{f}}}(s)$ of far user having high SNR $\gamma^{(j)}_{\mathrm{f}} \to \infty$ can be given with the aid of (5.21). To obtain a closed-form solution for the asymptotic BER expression $P_{\mathrm{f},\infty}(e)$, it is necessary to find a solution for the integral $\mathcal{I}^{(j)}_{\mathrm{f},\infty}\left(\frac{\pi}{2}\right)$, as presented in the Appendix C.

5.3.2.3 Asymptotic BER Expression for Near User n

For the near user n, the asymptotic BER expression is given by

$$\begin{aligned} P_{\mathrm{n},\infty}(e) = \mathcal{I}^{(1)}_{\mathrm{n},\infty}\left(\frac{\pi}{2}\right) + \frac{1}{4}\Big[-\mathcal{I}^{(2)}_{\mathrm{n},\infty}\left(\frac{\pi}{2}\right) + \mathcal{I}^{(3)}_{\mathrm{n},\infty}\left(\frac{\pi}{2}\right) \\ +\mathcal{I}^{(4)}_{\mathrm{n},\infty}\left(\frac{\pi}{2}\right) - \mathcal{I}^{(5)}_{\mathrm{n},\infty}\left(\frac{\pi}{2}\right)\Big], \end{aligned} \tag{5.24}$$

where $\mathcal{I}^{(j)}_{\mathrm{n},\infty}\left(\frac{\pi}{2}\right)$ is defined in a manner analogous to $\mathcal{I}^{(j)}_{\mathrm{f},\infty}\left(\frac{\pi}{2}\right)$, i.e.,

$$\mathcal{I}^{(j)}_{\mathrm{n},\infty}\left(\frac{\pi}{2}\right) = \frac{1}{\pi}\int_0^{\frac{\pi}{2}} M^{\infty}_{\gamma^{(j)}_{\mathrm{n}}}\Big(\frac{1}{2\sin^2\varphi}\Big)d\varphi, \tag{5.25}$$

where the asymptotic MGF expression $M^{\infty}_{\gamma^{(j)}_{\mathrm{n}}}(s)$ of near user n having high SNR $\gamma^{(j)}_{\mathrm{n}} \to \infty$ is given by using (5.21). Note that a solution of the integral $\mathcal{I}^{(j)}_{\mathrm{n},\infty}\left(\frac{\pi}{2}\right)$ is provided in Appendix C.

5.3.3 Diversity Order Analysis

The diversity order of user $\mathrm{u} \in \{\mathrm{n}, \mathrm{f}\}$ can be expressed as

$$\mathrm{O_u} = \lim_{\frac{\epsilon_\mathrm{u}}{N_0} \to \infty} \frac{-\log P_{\mathrm{u},\infty}(e)}{\log\left(\frac{\epsilon_\mathrm{u}}{N_0}\right)}. \tag{5.26}$$

By inserting (C.3) into either (5.22) or (5.24) and subsequently substituting the obtained asymptotic BER expression into (5.26), we arrive at a simplified diversity order expression, i.e.,

$$\mathrm{O_u} = N_\mathrm{u}. \tag{5.27}$$

It is worth mentioning that the diversity order of user $\mathrm{u} \in \{\mathrm{n}, \mathrm{f}\}$ is contingent upon the number of IRS elements, as one would expect.

5.4 Numerical and Simulation Results

In this section, we numerically compute the BER expressions for both the near user and the far user in order to analyze the considered downlink INOMA system over i.n.i.d Rician channels. We also present Monte Carlo simulations to validate the derived BER expressions. To simplify the presentation, we make the following assumptions for the parameters: $K_{h_\mathrm{u}} = K_1, K_{g_\mathrm{u}} = K_2, \alpha_{h_\mathrm{u}} = \alpha_1, \alpha_{g_\mathrm{u}} = \alpha_2$, and $d_{h_\mathrm{n}} = d_1, d_{g_\mathrm{n}} = d_2, d_{h_\mathrm{f}} = d_3, d_{g_\mathrm{f}} = d_4$. Additionally, the following parameter values are used for the numerical and simulation results, unless otherwise specified: total transmit power $P_\mathrm{t} = 1$, power coefficient $\alpha = 0.1$, distances in meters are $d_1 = d_2 =$ 10 m and $d_3 = d_4 = 20$ m, path loss exponents are $\alpha_1 = \alpha_2 = 2$, fading parameters

are $K_1 = K_2 = K = 10$, total number of IRS panels is $M = 2$, and the number of IRS elements in each IRS panel is $N_{\mathrm{m}} = 64$.

TABLE 5.1: Experimental values used for simulation and validation

Parameters	Values
Total transmit power (P_t)	1 Watt
Distance between BS to IRS-1 (d_1)	2 to 38 (meters)
Distance between BS to IRS-2 (d_3))	1 to 79 (meters)
Total distance between BS to Near user ($d_1 + d_2$)	20, 40 (meters)
Total distance between BS to Far user ($d_3 + d_4$)	40, 80 (meters)
Rician Fading parameter (K)	0, 5, 10
Number of IRS elements (N_m)	32, 64, 128
Power Coefficient (α)	0.1, 0.2, 0.3

Figure 5.2 depicts the BER performance of the IRS-assisted NOMA system with QPSK-BPSK modulation pair for the near user and the far user. The simulation results match closely with the analytical results, as shown in Figure 5.2. For the given set of parameters, the near user requires less transmit power since its channel strength is stronger than far user. Further, we observe that the BER performance of near user is better than the far user. For example, the near user has nearly 1.5 dB SNR gain at BER = 10^{-4} in comparison to the far user.

Figure 5.3 shows the BER performance as a function of SNR for the near user and the far user with varying the Rician fading parameter K. The simulation results are matching closely with analytical results. An increase in the Rician fading factor K represents the stronger LoS component present in the fading channels. Hence, as expected, there is a performance enhancement in the BER performance of both the users as we increase the value of K from 0 to 10. At the same time, we can also observe that there is not much improvement in the BER performance of both the users when the value of K is changing from 5 to 10.

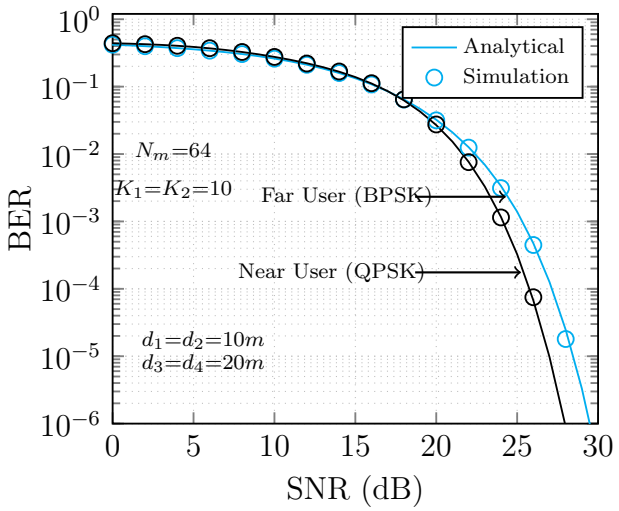

FIGURE 5.2: BER w.r.t SNR performance of near and far users for fixed $N_m = 64$. The solid lines and marker denote the analytical and simulation results, respectively.

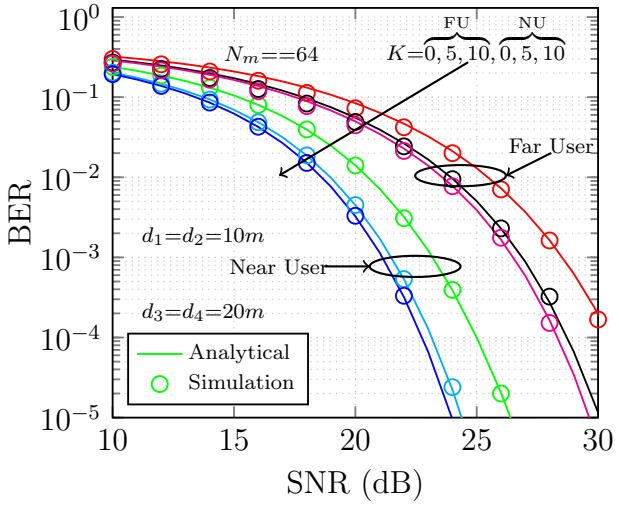

FIGURE 5.3: BER performance w.r.t SNR (dB) with varying the fading parameter K. The solid lines and marker denote the analytical and simulation results, respectively.

Figure 5.4 depicts the BER performance as a function of SNR for the near user and the far user with varying the number of IRS elements N_u. The simulation results are matching closely with analytical results. As we increase the N_u from 32 to 128, the BER performance of both the users will shift together towards the left-hand side. For a fixed BER of 10^{-4} both the user has a BER performance improvement in SNR

of 10 dB if we increase the N_u from 32 to 128.

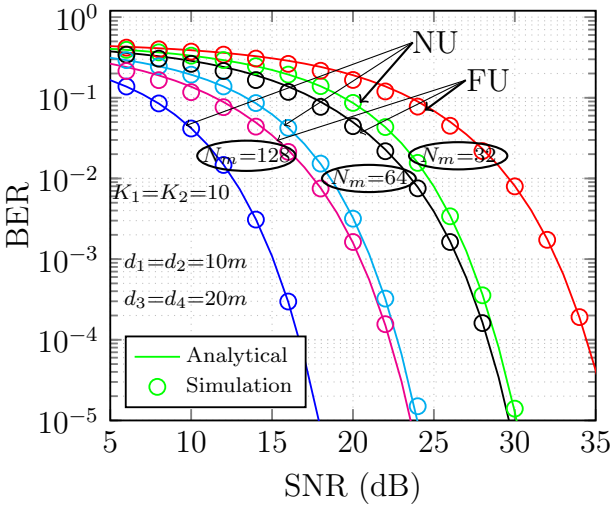

FIGURE 5.4: BER performance with varying the number of IRS elements in the panels $N_m = 32, 64, 128$. The solid lines and marker denote the analytical and simulation results, respectively.

Figure 5.5 shows the BER performance as a function of SNR for the near and the far users with varying the power coefficient α. The simulation results are matching closely with the analytical results. As we are increasing the value of α from 0.1 to 0.3 there is a BER performance improvement for the near user, whereas BER performance degrades for the far user. For a fixed BER of 10^{-4} there is a BER performance improvement of 5 dB for near user whereas there is a BER decline of 6 dB for the far user if we increase the value of α from 0.1 to 0.3. Since power of the far user is $\epsilon_f = (1 - \alpha)P_t$.

Next, Figure 5.6 illustrates the impact of a position (d_1) of the IRS-1 from the BS on the BER performance of the near user. The total distance of the user from the BS is assumed to be $d_1 + d_2 = 40$ m. It can be noticed that the BER performance improves for the near user if the IRS panel is placed closer to either BS or the near user. The reason is that the IRS panels placed closer to either BS or the near user have a small path loss. Thus, it can provide reliable communication. The

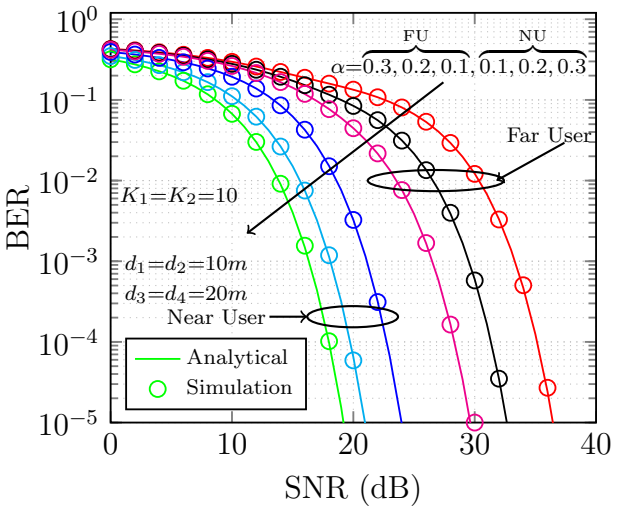

FIGURE 5.5: BER performance w.r.t. SNR (dB) with varying the near use power coefficient α. The solid lines and marker denote the analytical and simulation results, respectively.

BER performance of the near user is symmetric about the equidistant position i.e., $d_1 = 20$ m and the BER performance is worst at the equidistant position. Similarly, Figure 5.7 illustrates the impact of a position (d_3) of the IRS-2 from the BS on the BER performance of the far user. The total distance of the user from the BS is assumed to $d_3 + d_4 = 80$ m. It can be noticed that the BER performance improves for the far user if IRS-2 is placed closer to either BS or the far user. The reason is that the IRS panels placed closer to either BS or the near user have small path loss, thus it can provide reliable communication. The BER performance of the near user is symmetric about the equidistant position, i.e., $d3 = 40$ m and the BER performance is worst at the equidistant position.

5.5 Conclusion

We have conducted a comprehensive study of the BER performance in an IRS-assisted downlink power domain NOMA system, considering i.n.i.d. Rician fading

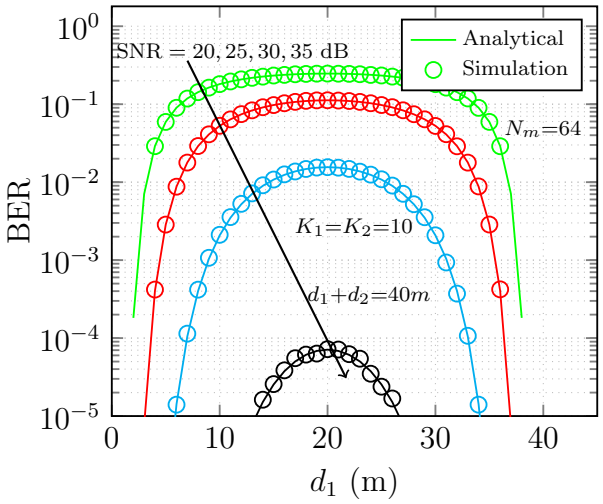

FIGURE 5.6: BER performance of near user w.r.t distance d_1 with varying SNR. The solid lines and marker denote the analytical and simulation results, respectively.

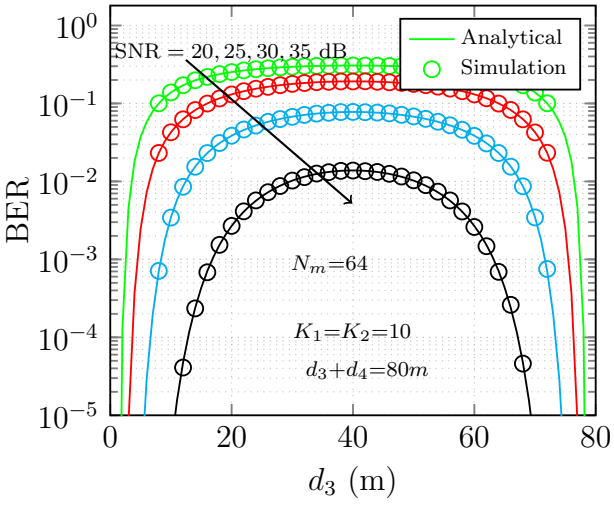

FIGURE 5.7: BER performance of far user w.r.t distance d_3 (in meters) with varying SNR. The solid lines and marker denote the analytical and simulation results, respectively.

channels and SIC errors. We have obtained closed-form BER expressions for both near and far users, considering a substantial number of IRS elements. Furthermore, we have also obtained asymptotic BER expressions for each user. Our investigation further has examined the impact of various factors, such as the fading parameter, number of IRS elements, power coefficient of the near user, and location of IRS

panels, on the BER performance of both near and far users. The precision of our theoretical analysis is confirmed through extensive Monte Carlo simulations, and the results reveal a substantial enhancement in BER performance as the number of reflecting elements increases.